Apoptosis of Insulin-Secreting Cells Induced by Endoplasmic Reticulum Stress Is Amplified by Overexpression of Group VIA Calcium-Independent Phospholipase A_2 (iPLA$_2\beta$) and Suppressed by Inhibition of iPLA$_2\beta$[†]

Sasanka Ramanadham,*[,‡] Fong-Fu Hsu,[‡] Sheng Zhang,[‡] Chun Jin,[‡] Alan Bohrer,[‡] Haowei Song,[‡] Shunzhong Bao,[‡] Zhongmin Ma,[§] and John Turk[‡]

Mass Spectrometry Resource, Division of Endocrinology, Diabetes, and Metabolism, Department of Medicine, Washington University School of Medicine, Box 8127, 660 South Euclid Avenue, St. Louis, Missouri 63110, and Mount Sinai School of Medicine, New York, New York 10029

Received August 27, 2003; Revised Manuscript Received November 18, 2003

ABSTRACT: The death of insulin-secreting β-cells that causes type I diabetes mellitus (DM) occurs in part by apoptosis, and apoptosis also contributes to progressive β-cell dysfunction in type II DM. Recent reports indicate that ER stress-induced apoptosis contributes to β-cell loss in diabetes. Agents that deplete ER calcium levels induce β-cell apoptosis by a process that is independent of increases in $[Ca^{2+}]_i$. Here we report that the SERCA inhibitor thapsigargin induces apoptosis in INS-1 insulinoma cells and that this is inhibited by a bromoenol lactone (BEL) inhibitor of group VIA calcium-independent phospholipase A_2 (iPLA$_2\beta$). Overexpression of iPLA$_2\beta$ amplifies thapsigargin-induced apoptosis of INS-1 cells, and this is also suppressed by BEL. The magnitude of thapsigargin-induced INS-1 cell apoptosis correlates with the level of iPLA$_2\beta$ expression in various cell lines, and apoptosis is associated with stimulation of iPLA$_2\beta$ activity, perinuclear accumulation of iPLA$_2\beta$ protein and activity, and caspase-3-catalyzed cleavage of full-length 84 kDa iPLA$_2\beta$ to a 62 kDa product that associates with nuclei. Thapsigargin also induces ceramide accumulation in INS-1 cells, and this response is amplified in cells that overexpress iPLA$_2\beta$. These findings indicate that iPLA$_2\beta$ participates in ER stress-induced apoptosis, a pathway that promotes β-cell death in diabetes.

Diabetes mellitus (DM)[1] is the most prevalent human endocrine disease, and it results from loss and/or dysfunction of insulin-secreting β-cells in pancreatic islets. Type I DM is caused by autoimmune β-cell destruction (*1*−*3*), and type II DM results from a progressive decline of β-cell function in the context of insulin resistance (*4*, *5*). Apoptosis contributes to β-cell loss in both type I DM (*6*) and type II DM (*7*−*12*).

Insulin resistance that occurs in rodent models of obesity and in obese humans is associated with an adaptive increase in β-cell mass (*13*−*17*). Autopsy studies indicate that the β-cell mass in obese type II DM patients is smaller than that in obese nondiabetic subjects (*17*−*19*). The reduction in β-cell mass that occurs in the ZDF rat model of type II DM and in human type II DM patients appears not to be attributable to a reduced level of β-cell proliferation or neogenesis but to an increased level of β-cell death by apoptosis (*20*, *21*).

It is therefore important to understand the mechanisms underlying β-cell apoptosis if this process is to be prevented or retarded. Several stimuli induce β-cell apoptosis (*22*) by incompletely understood mechanisms. Three currently recognized apoptotic signaling pathways are the extrinsic death receptor pathway, the intrinsic mitochondrial pathway, and the endoplasmic reticulum (ER) stress pathway (*23*, *24*).

ER stress from the loss of Ca^{2+} stores is induced by the SERCA inhibitor thapsigargin (*25*), and this agent induces insulinoma cell apoptosis by a pathway that does not require an increase in the cytosolic Ca^{2+} concentration but that does require the generation of arachidonic acid 12-lipoxygenase products (*26*). Thapsigargin-induced ER stress in isolated pancreatic islets is associated with hydrolysis of arachidonic acid from membrane phospholipids by a calcium-independent

[†] This research was supported in part by grants from the National Institutes of Health (R37-DK34388, P41-RR00954, P01-HL57278, P60-DK20579, and P30-DK56341) and by an Award (to S.R.) from the American Diabetes Association.

* To whom correspondence should be addressed: Department of Medicine, Washington University School of Medicine, Box 8127, 660 S. Euclid Ave., St. Louis, MO 63110. Phone: (314) 362-8194. Fax: (314) 362-8188. E-mail: sramanad@im.wustl.edu.

[‡] Washington University School of Medicine.

[§] Mount Sinai School of Medicine.

[1] Abbreviations: AA, arachidonic acid; BEL, bromoenol lactone suicide inhibitor of iPLA$_2\beta$; BME, β-mercaptoethanol; BSA, bovine serum albumin; CAD, collisionally activated dissociation; CM, ceramide; CNL, constant neutral loss; C3-I, caspase-3 inhibitor; cPLA$_2$, group IV cytosolic phospholipase A_2; ECL, enhanced chemiluminescence; EGFP, enhanced green fluorescence protein; ER, endoplasmic reticulum; ESI, electrospray ionization; FBS, fetal bovine serum; IF, immunocytofluorescence; iPLA$_2\beta$, β-isoform of group VIA calcium-independent phospholipase A_2; IS, internal standard; MS, mass spectrometry; OE, iPLA$_2\beta$-overexpressing cells; O/N, overnight; PAGE, polyacrylamide gel electrophoresis; PBS, phosphate-buffered saline; PIC, protease inhibitor cocktail; PLA$_2$, phospholipase A_2; SDS, sodium dodecyl sulfate; SEM, standard error of the mean; SERCA, sarcoendoplasmic reticulum Ca^{2+}-ATPase; TBS-T, Tris-buffered saline-tween; TIC, total ion current; TLC, thin-layer chromatography; TUNEL, terminal deoxynucleotidyl transferase-mediated (fluorescein) dUTP nick end labeling; RT, room temperature; RT-PCR, reverse transcription polymerase chain reaction.

10.1021/bi035536m CCC: $27.50
Published on Web 01/08/2004

mechanism that is suppressed by a bromoenol lactone (BEL) inhibitor of group VIA calcium-independent phospholipase A$_2\beta$ (iPLA$_2\beta$) (*27*). These observations suggest that iPLA$_2\beta$ participates in ER stress-induced β-cell apoptosis.

A role for iPLA$_2\beta$ in apoptosis is also suggested by the finding that induction of apoptosis of human U937 promonocytes by anti-Fas antibody is associated with hydrolysis of arachidonic acid from membrane phospholipids by a mechanism that is inhibited by BEL and that is not catalyzed by sPLA$_2$ or cPLA$_2$ (*28*). U937 cell apoptosis is also associated with cleavage of iPLA$_2\beta$ by caspase-3 (*29*), a protease that is central to apoptosis execution. Overexpression of this iPLA$_2\beta$ cleavage product in kidney cells amplifies both thapsigargin-induced arachidonate release and cell death (*29*), raising the possibility that the caspase-3 cleavage product of iPLA$_2\beta$ is involved in apoptosis.

Collectively, these observations (*26*−*29*) suggest that iPLA$_2\beta$ might participate in ER stress-induced β-cell apoptosis, and therefore, the effects of overexpression and of inhibition of iPLA$_2\beta$ on this process were examined here.

MATERIALS AND METHODS

Materials. INS-1 β-cells were generously provided by C. Newgard (Duke University Medical Center, Durham, NC). Other materials were obtained from the following sources: (16:0/[^{14}C]-18:2)GPC (PLPC, 55 mCi/mmol), rainbow molecular mass standards and enhanced chemiluminescence (ECL) reagent (Amersham Biosciences, Arlington Heights, IL), ceramide and other lipid standards (Avanti Polar Lipids, Alabaster, AL), sodium dodecyl sulfate−polyacrylamide gel electrophoresis (SDS−PAGE) supplies and Triton X-100 (Bio-Rad, Hercules, CA), retroviral vector (Clontech, Palo Alto, CA), paraformaldehyde (Electron Microscopy Sciences, Ft. Washington, PA), TLC solvents (Fisher, Pittsburgh, PA), RT-PCR reagents (Invitrogen, Carlsbad, CA), normal goat serum and Cy3-conjugated affinipure goat anti-rabbit IgG (H+L) (Jackson Immuno Research Laboratories, West Grove, PA), pentex fraction V fatty acid-free bovine serum albumin (ICN Biomedicals Inc., Aurora, OH), Slow Fade light antifade kit (Molecular Probes, Eugene, OR), caspase-3 inhibitor IV (C3-I, Oncogene Research Products, Boston, MA), Coomasie reagent (Pierce, Rockford, IL), peroxidase-conjugated goat anti-rabbit IgG antibody and TUNEL and DNA Laddering kits (Roche Diagnostic Corp., Indianapolis, IN), and common reagents and salts (Sigma Chemical Co., St. Louis, MO).

Preparation of and Culture of Stably Transfected INS-1 Cells Overexpressing Islet iPLA$_2\beta$. A retroviral system (*30*, *31*) was used to stably transfect INS-1 cells with either empty retroviral vector (V) or a vector construct containing iPLA$_2\beta$ cDNA, as described previously (*32*). The INS-1 cells were cultured, as described previously (*33*), and grown to confluency in Petri dishes or flasks prior to being treated with thapsigargin (1 μM).

Preparation of iPLA$_2\beta$ as a Fusion Protein with EGFP. EGFP-N2 and EGFP-C2 vectors (*34*) and constructs encoding EGFP and iPLA$_2\beta$ cDNA were transfected into INS-1 cells with a Gene PORTER transfection system (Gene Therapy Systems, San Diego, CA). To select stably transfected cells that express EGFP or fusion proteins of iPLA$_2\beta$-EGFP (N2) or EGFP-iPLA$_2\beta$ (C2), the selection agent G418 (0.4 mg/mL) was added to culture medium for 2 weeks. Fluorescence-activated cell sorting was then used to increase the efficiency of the selection.

Treatment of Cells and Assessment of Apoptosis. The INS-1 cells were treated with vehicle (DMSO) alone or with thapsigargin (1 μM) in the absence and presence of inhibitors for up to 24 h. Induction of INS-1 cell apoptosis was then assessed by TUNEL and DNA laddering analyses, performed according to the manufacturer's instructions.

Preparation of INS-1 Cell Subcellular Fractions and the iPLA$_2\beta$ Activity Assay. INS-1 cell cytosol and membrane fractions (*35*) and nuclear enriched fractions (*33*) were prepared as described previously. The purity of the nuclear fraction, using organelle specific assays (*36*, *37*), and the presence of iPLA$_2\beta$ activity (*38*, *39*) in this fraction were verified, as described previously (*33*). The Ca^{2+}-independent PLA$_2\beta$ activity in aliquots of cellular fractions (30 μg of protein) was assayed in the presence of 1-palmitoyl-2-[^{14}C]-linoleoyl-*sn*-glycero-3-phosphocholine (PLPC, 5 μM) as the substrate, and specific enzymatic activity was quantitated, as described previously (*35*, *40*).

Immunoblotting and Immunocytofluorescence Analyses of INS-1 Cell iPLA$_2\beta$ Protein. INS-1 cell protein was analyzed by SDS−PAGE (7.5%), transferred onto Immobilon-P PVDF membranes, and processed for immunoblotting analyses, and iPLA$_2\beta$-immunoreactive protein bands were visualized by enhanced chemiluminescence (ECL), as described previously (*33*). Cellular localization of iPLA$_2\beta$ protein was achieved using an immunocytofluorescence staining protocol. Following removal of media, cells seeded in chambered glass slides were washed, fixed, permeabilized, and sequentially incubated with iPLA$_2\beta$ primary antibodies (0.003 μg/μL) and with fluorescent Cy3-conjugated AffiniPure goat anti-rabbit IgG secondary antibody (1:400, 1 h), as described previously (*33*). Cellular iPLA$_2\beta$ immunocytofluorescence was then visualized by fluorescence microscopy at an excitation wavelength of 550 nm and an emission wavelength of 570 nm.

Ceramide Analyses. Phospholipids were extracted from INS-1 cells under acidic conditions [2/2/1.8 (v/v/v) chloroform/methanol/2% acetic acid mixture] as described previously (*41*, *42*). An aliquot of the chloroform layer was saved for PO_4 quantitation. To the organic layer was added C8-ceramide (C8-CM) internal standard (IS, 500 ng), and the mixture was concentrated to dryness under nitrogen. The sample was then analyzed by silica gel G TLC [65/25/4 (v/v/v) chloroform/methanol/30% ammonium hydroxide mixture]. The ceramide standard-containing region was identified with phosphomolybdate staining and ceramide extracted in the presence of 0.6% LiCl to facilitate formation of Li^+ adducts, as described previously (*43*, *44*). Samples were concentrated and then reconstituted in a 1/4 chloroform/methanol mixture containing 10 pmol/μL LiOH.

To measure ceramide content, ESI/MS/MS standard curves were generated from a series of samples containing a fixed amount of C8-CM standard and varied amounts of long chain CM standards. The amounts of individual CM species relative to the C8-CM internal standard were measured by ESI/MS/MS scanning for a constant neutral loss (CNL) of 48, which reflects the elimination of formaldehyde and water from the $[M + Li^+]^+$ ion (*45*). This loss is characteristic of CM−Li^+ adducts upon low-energy collisionally activated

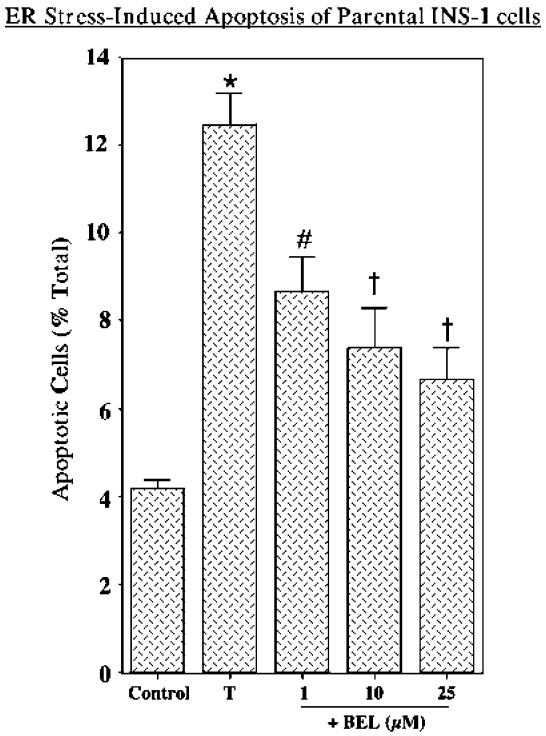

FIGURE 1: ER stress-induced apoptosis in parental INS-1 cells and effects of BEL inhibition. Parental INS-1 cells were treated with either vehicle (DMSO) alone (Control) or 1 μM thapsigargin (T) in the absence and presence of 1, 10, or 25 μM BEL. After 24 h, the cells were harvested for TUNEL analyses. The data representing the percentage of apoptotic cells, relative to the total number of cells, are illustrated as the mean ± SEM ($n = 5$). The asterisk denotes that the thapsigargin-treated group is significantly different from the control group ($p < 0.01$). The pound sign denotes that the BEL-treated group is significantly different from the T and Control groups ($p < 0.01$). The daggers denote that the BEL-treated group is significantly different from the T group ($p < 0.05$).

dissociation (CAD) ESI/MS/MS (*41*). Sample contents of the various CM species were expressed relative to lipid phosphorus, which was measured as described previously (*46*).

Statistical Analyses. Data were converted to mean ± SEM values where appropriate, and the Student's *t* test was applied to determine significant differences between members of a pair ($p < 0.05$). Statistical differences between multiple treatment groups and a control group were determined using analysis of variances and the Dunnett post-hoc test.

RESULTS

ER Stress-Induced Apoptosis of Parental INS-1 Cells. To examine the effects of ER stress on INS-1 insulinoma cells, nontransfected parental INS-1 cells were treated with vehicle (DMSO) alone or with thapsigargin, and induction of apoptosis was assessed by TUNEL analyses. Figure 1 illustrates that induction of ER stress with thapsigargin induces a 3-fold increase in the level of apoptosis in parental INS-1 cells. This was attenuated by BEL, an inhibitor of iPLA$_2\beta$, suggesting that iPLA$_2\beta$ might be involved in ER stress-induced apoptosis.

Amplification of ER Stress-Induced Apoptosis in Stably Transfected INS-1 Cells that Overexpress iPLA$_2\beta$ (OE). The possible nonspecificity of pharmacologic inhibitors such as BEL (*47*, *48*) caused us to pursue a molecular biologic

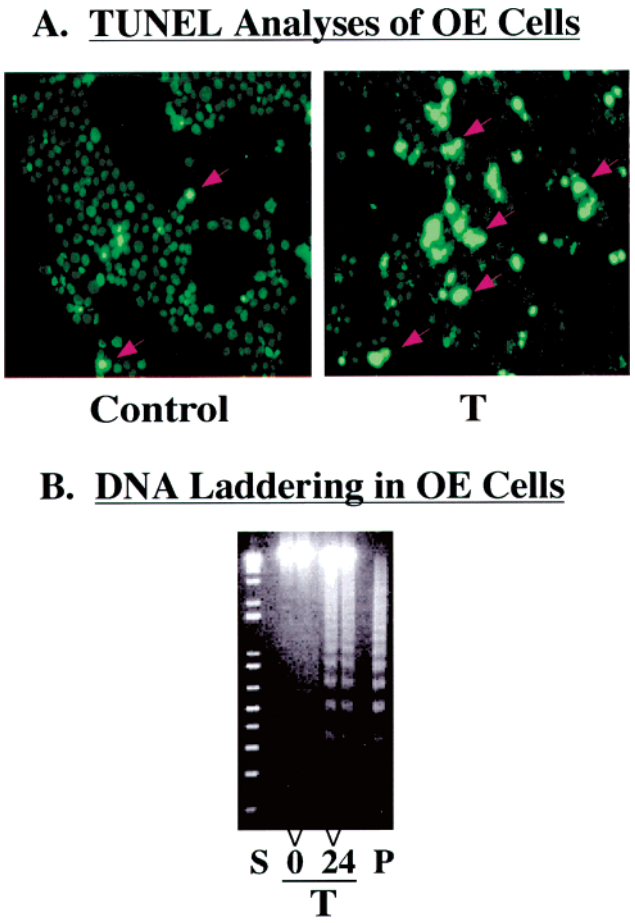

FIGURE 2: ER stress-induced apoptosis of iPLA$_2\beta$-overexpressing INS-1 cells. Stably transfected INS-1 cells that overexpress iPLA$_2\beta$ (OE) were treated with vehicle alone (Control) or with thapsigargin (T, 1 μM). After 24 h, the cells were harvested for TUNEL and DNA laddering analyses to determine the fraction of the cell population undergoing apoptosis. (A) The brightly fluorescent cells, denoted with red arrows, reflect apoptotic cells. (B) The lanes marked 0 and 24 contain DNA from OE cells that were treated with thapsigargin for 0 and 24 h, respectively. Lane S contained the standard kilobase ladder, and lane P contained the standard positive sample of DNA from U937 cells provided by the manufacturer.

approach in further examining the role of iPLA$_2\beta$ in apoptosis by manipulating INS-1 cellular levels of iPLA$_2\beta$ activity. Antisense approaches are ineffective in reducing INS-1 cell iPLA$_2\beta$ activity (*45*), but stable transfection with retroviral vectors containing iPLA$_2\beta$ cDNA has produced several clonal lines that overexpress iPLA$_2\beta$ (*45*). Such INS-1 cell lines overexpressing iPLA$_2\beta$ (OE) were used to further examine the role of iPLA$_2\beta$ in ER stress-induced apoptosis.

A greater fraction of OE cells subjected to ER stress are TUNEL positive (Figure 2A, right panel) compared to vehicle-treated control OE cells (Figure 2A, left panel). Similarly, ER stress induces a time-dependent increase in the level of DNA laddering in OE cells (Figure 2B). Thus, both the parental INS-1 cell line (Figure 1) and stably transfected INS-1 cells that overexpress iPLA$_2\beta$ (Figure 2) undergo apoptosis when subjected to ER stress induced by thapsigargin.

Quantitative analyses indicate that a greater fraction of iPLA$_2\beta$-overexpressing (OE) INS-1 cells undergo apoptosis when subjected to ER stress, relative to vehicle-treated cells, than is the case for INS-1 cells transfected with an empty

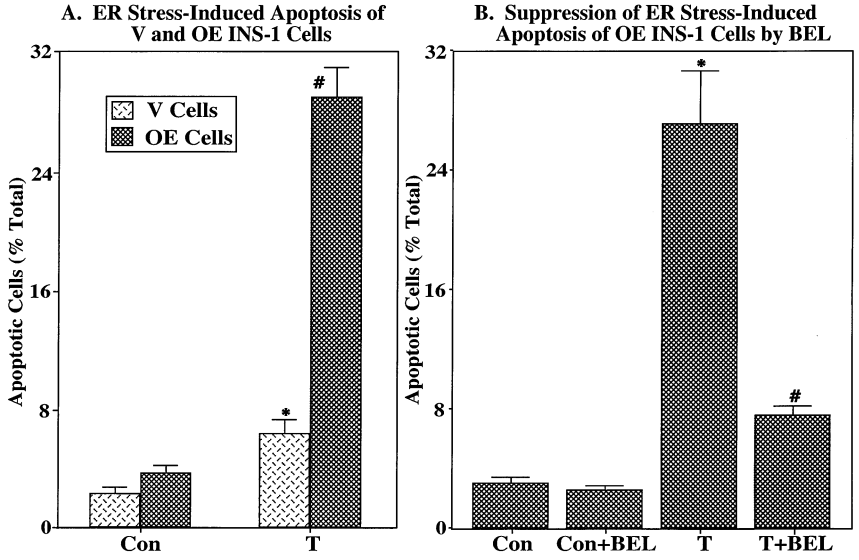

FIGURE 3: Effects of iPLA$_2\beta$ inhibition on ER stress-induced apoptosis in stably transfected INS-1 cells that overexpress iPLA$_2\beta$. (A) Stably transfected INS-1 cells that overexpress iPLA$_2\beta$ (OE cells) or cells that were transfected with the empty retroviral vector (V cells) that contained no iPLA$_2\beta$ cDNA were treated with vehicle alone (Con) or with thapsigargin (T, 1 μM). After 24 h, the fraction of apoptotic cells was determined with a TUNEL assay. The asterisk denotes that T-treated V cells are significantly different from the corresponding Con group and the pound sign that T-treated OE cells are significantly different from all groups ($p < 0.05$). (B) OE cells were cultured with vehicle alone (Con) or with thapsigargin (T, 1 μM) in the absence and presence of BEL (1 μM). The asterisk denotes that the T-treated group is significantly different from the Con groups ($p < 0.05$) and the pound sign that the T- and BEL-treated group is significantly different from other groups ($p < 0.05$). The data representing the percentage of apoptotic cells, relative to the total number of cells, are illustrated as the mean ± SEM ($n = 19$).

retroviral vector (V) that contained no iPLA$_2\beta$ cDNA (Figure 3A). Chelation of extracellular and/or intracellular Ca^{2+} with EGTA and/or BATPA-AM, respectively, does not affect the fraction of OE cells that become apoptotic after being subjected to ER stress (not shown). However, inhibition of iPLA$_2\beta$ activity with BEL, while not affecting control levels of apoptosis over a 24 h period, greatly reduces the level of ER stress-induced OE cell apoptosis (Figure 3B). These findings support the possibility that iPLA$_2\beta$ participates in ER stress-induced β-cell apoptosis.

Correlation between the iPLA$_2\beta$ Expression Level and Apoptosis in INS-1 Cell Lines Subjected to ER Stress. The potential involvement of iPLA$_2\beta$ in ER stress-induced apoptosis was further examined by comparing the fraction of cell populations that develop apoptosis among several INS-1 cell lines expressing varying levels of iPLA$_2\beta$ activity. Figure 4 illustrates that among five such cell lines studied there is a monotonically increasing relationship between the level of iPLA$_2\beta$ specific activity and the fraction of the INS-1 cell population that is apoptotic after induction of ER stress with thapsigargin. The level of iPLA$_2\beta$-immunoreactive protein as assessed by Western blotting analyses correlates well with the level of iPLA$_2\beta$ activity (Figure 4, inset).

Changes in the Subcellular Distribution of iPLA$_2\beta$ Activity after Induction of ER Stress. Membrane-associated iPLA$_2\beta$ specific activity exhibits a time-dependent increase for the first 12 h after induction of ER stress and then declines over the next 12 h (Figure 5A). During the first 6 h after induction of ER stress, iPLA$_2\beta$ specific activity declines in cytosol (Figure 5A) and there is a parallel rise in iPLA$_2\beta$ activity associated with the nuclear subcellular fraction (Figure 5B). The iPLA$_2\beta$ activity associated with nuclei then declines over the next 8 h, while that in cytosol rises to a peak at 16 h and then declines.

Changes in the Subcellular Distribution of the iPLA$_2\beta$-Immunoreactive Protein after Induction of ER Stress. Immunocytofluorescence analyses indicate that under control resting conditions iPLA$_2\beta$-immunoreactive protein is dispersed in the cytosol of OE cells, and there is a light perinuclear halo (Figure 6A, left panel). Induction of ER stress with thapsigargin causes a marked increase in iPLA$_2\beta$ perinuclear fluorescence (Figure 6A, right panel). This is associated with a stronger signal for iPLA$_2\beta$-immunoreactive protein bands with apparent SDS−PAGE molecular masses of 84, 70, and 62 kDa in the nuclear fraction of OE cells after induction of ER stress with thapsigargin (Figure 6B). The identity of iPLA$_2\beta$-immunoreactive protein on such SDS−PAGE gels as authentic iPLA$_2\beta$ isoforms has recently been confirmed by mass spectrometric analyses.[2] The relative intensity of the 62 kDa iPLA$_2\beta$-immunoreactive band exhibits the greatest increase of the three major distinguishable bands.

Further Characterization of the 62 kDa iPLA$_2\beta$-Immunoreactive Protein that Accumulates in INS-1 Cells Subjected to ER Stress. The iPLA$_2\beta$ deduced amino acid sequence contains a consensus sequence (^{180}DVTD^{183}) for cleavage by caspase-3, and caspase-3 is activated during apoptosis (*29*). Cleavage of rat iPLA$_2\beta$ at this site would yield a 62 kDa product that retains the ^{462}GTSTG^{466} serine lipase catalytic center (*31*). We thus postulated that the 62 kDa iPLA$_2\beta$-immunoreactive protein that accumulates in the nuclear fraction of INS-1 cells undergoing apoptosis represents the caspase-3 cleavage product of iPLA$_2\beta$ (N^{184}−P^{752}).

The iPLA$_2\beta$ antibody preparation used in these studies was generated by multiple-antigen core technology (Invitrogen)

[2] Ramanadham, S., Song, H., Hsu, F.-F., Zhang, S., Chankshaw, M., Grant, G. A, Newgard, C. B., Bao, S., Ma, Z., and Turk, J. (2003) *Biochemistry 42* (47), 13929−13940.

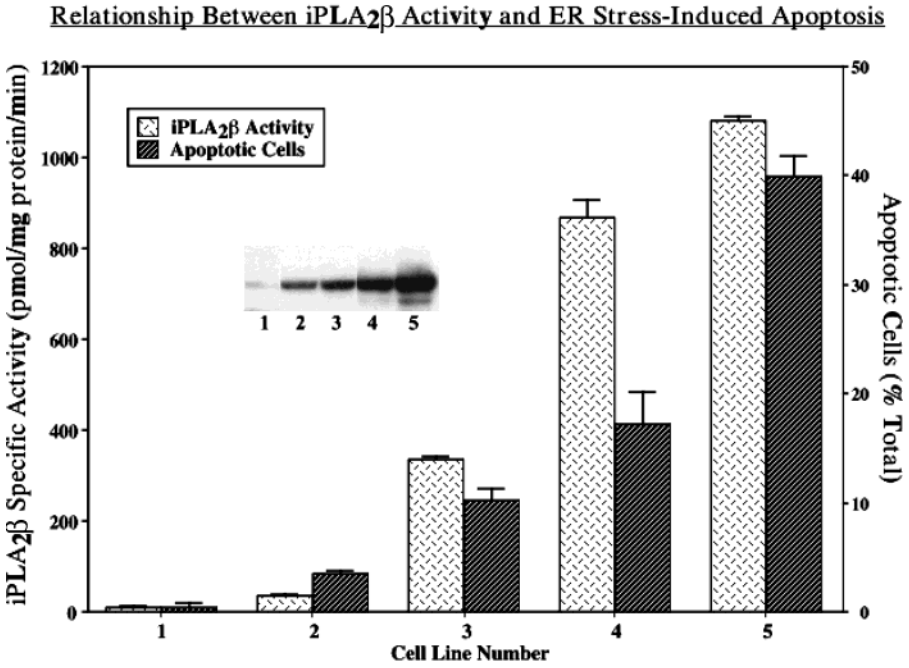

FIGURE 4: Relationship between iPLA$_2\beta$ activity and ER stress-induced INS-1 cell apoptosis. Five distinct INS-1 cell lines that overexpressed varied levels of iPLA$_2\beta$ activity were treated with thapsigargin (1 μM). After 24 h, the cells were harvested and processed for iPLA$_2\beta$ activity and TUNEL analyses. The data representing the specific iPLA$_2\beta$ enzymatic activity and the percentage of apoptotic cells, relative to the total number of cells, are illustrated as the mean ± SEM ($n = 6$). The inset shows iPLA$_2\beta$ immunoblotting analyses in 30 μg protein aliquots of homogenates prepared from the five INS-1 cell lines.

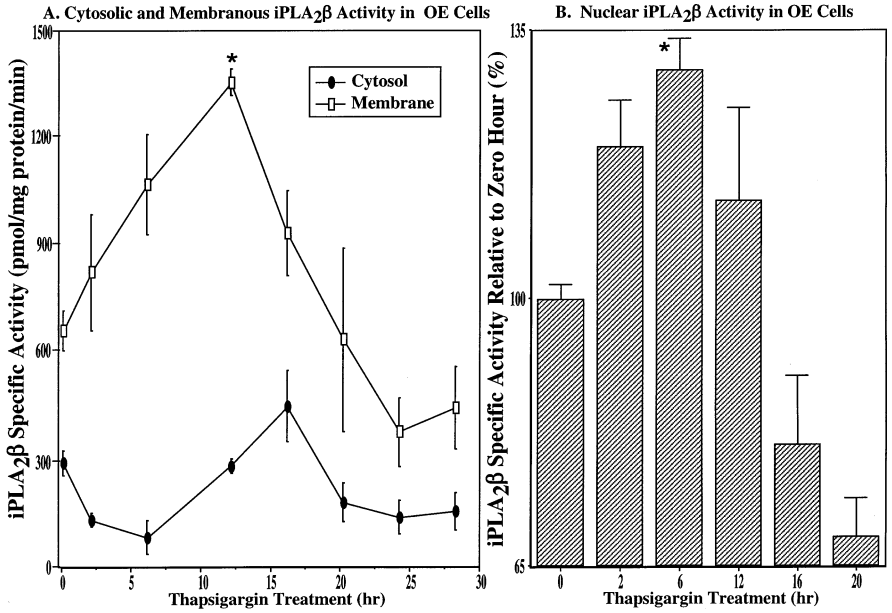

FIGURE 5: ER stress-induced changes in the subcellular distribution of iPLA$_2\beta$ activity. (A) Aliquots (containing 30 μg of protein) of cytosol and resuspended membranes prepared from OE cells, as described previously (*35*), were assayed for iPLA$_2\beta$ activity at various times following treatment with thapsigargin (1 μM). The data are presented as the mean ± SEM ($n = 19$). The asterisk denotes that the thapsigargin-treated group is significantly different from the 0 h group ($p < 0.05$). (B) The nuclear fraction was prepared, as described previously (*33*), from OE cells treated with thapsigargin for various intervals. The data are presented as the mean ± SEM ($n = 19$) of the percent change in enzymatic activity following thapsigargin treatment, relative to 0 h values. The asterisk denotes that the thapsigargin-treated group is significantly different from the 0 h group ($p < 0.05$).

using two peptides [(1) $K^{25}-E^{41}$ and (2) $M^{589}-S^{502}$] (Figure 7A) from the rat iPLA$_2\beta$ deduced amino acid sequence (*31*). Inclusion of both peptides in incubations with the iPLA$_2\beta$ antibody blocks recognition of iPLA$_2\beta$ by competing for and saturating the antibody binding sites. Either peptide alone fails to prevent recognition of full-length iPLA$_2\beta$ by the iPLA$_2\beta$ antibody preparation. Since the postulated 62 kDa iPLA$_2\beta$ caspase-3 cleavage product $N^{184}-P^{752}$ lacks the region of sequence recognized by peptide 1, we postulated that peptide 2, but not peptide 1, alone would block recognition of the 62 kDa iPLA$_2\beta$-immunoreactive protein by the iPLA$_2\beta$ antibody preparation (Figure 7A).

Consistent with an origin from caspase-3 action, cellular production of the 62 kDa iPLA$_2\beta$-immunoreactive protein

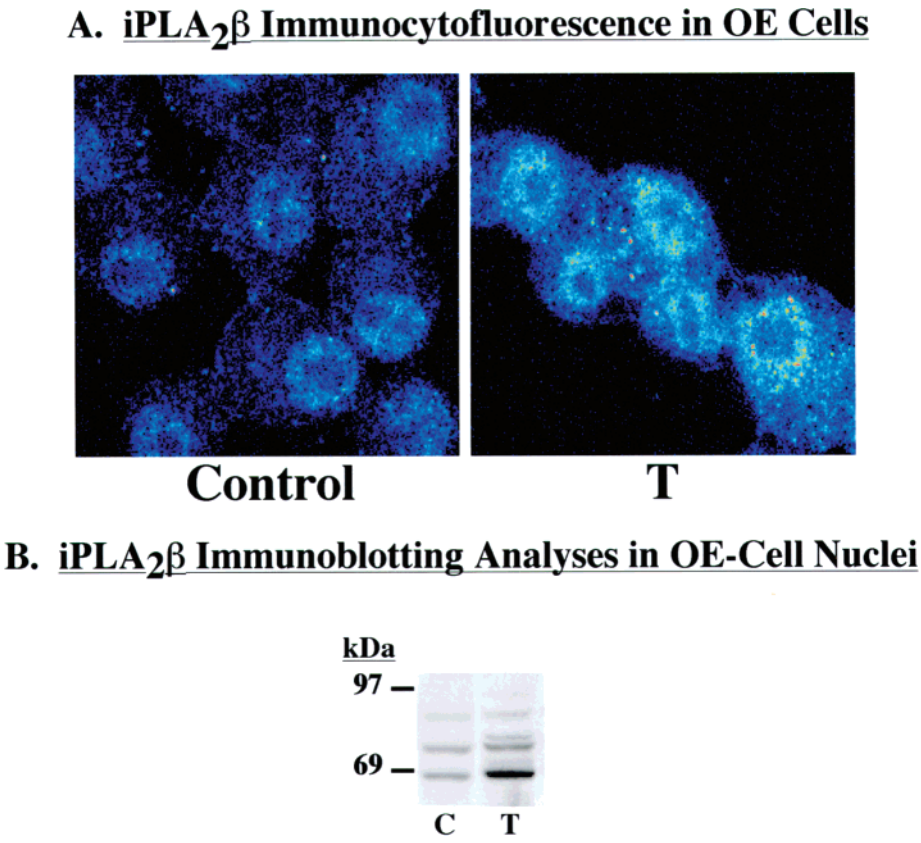

FIGURE 6: Changes in the subcellular distribution of iPLA$_2\beta$-immunoreactive protein after induction of ER stress in INS-1 cells. (A) Cells seeded in glass-chambered slides were cultured in the presence of a vehicle alone or thapsigargin (T, 1 μM) for 24 h and then processed for immunocytofluorescence analyses. Fixed, permeabilized cells were probed with polyclonal iPLA$_2\beta$ antibodies followed by visualization of Cy3 fluorescence. (B) Aliquots of the INS-1 cell nuclear protein (50 μg) prepared from OE cells treated with thapsigargin (1 μM) were analyzed by SDS−PAGE (7.5%) and transferred onto Immobilon-P PVDF membranes. The electroblot was probed with iPLA$_2\beta$ antibodies, and immunoreactive protein bands were visualized by enhanced chemiluminescence (ECL): vehicle-treated controls (C) and thapsigargin-treated cells (T).

(Figure 7B, lane 1) is blocked by a caspase-3 inhibitor (C3-I, Figure 7B, lane 2). Recognition of the 62 kDa iPLA$_2\beta$-immunoreactive protein is also blocked by peptide 2 (Figure 7B, lane 3) but unaffected by peptide 1 (not shown). However, neither the production of (Figure 7B, lanes 1 and 2) nor the recognition of (Figure 7B, lanes 1 and 3) the 70 and 84 kDa iPLA$_2\beta$-immunoreactive proteins is affected by C3-I and peptide 2, respectively. These observations are consistent with the scheme proposed in Figure 7A in which the 62 kDa iPLA$_2\beta$-immunoreactive protein represents the caspase-3 cleavage product ($N^{184}-P^{752}$) of iPLA$_2\beta$ and contains the sequence represented by peptide 2 but not that represented by peptide 1, while the 70 and 84 kDa iPLA$_2\beta$-immunoreactive proteins retain the region of sequence represented by peptide 1.

A similar antigen blocking strategy was employed to gain information about the subcellular distribution of the iPLA$_2\beta$-immunoreactive protein in immunocytofluorescence studies (Figure 7C). INS-1 cells probed with the iPLA$_2\beta$ antibody preparation alone exhibit immunocytofluorescence dispersed in cytoplasm with a perinuclear halo (Figure 7C, panel a). Inclusion of both antigen peptides 1 and 2 in the incubations with iPLA$_2\beta$ antibody markedly reduces both cytoplasmic and perinuclear fluorescence (Figure 7C, panel d). Antigen peptide 2 alone (Figure 7C, panel b) but not antigen peptide 1 alone (Figure 7C, panel c) suppresses visualization of perinuclear immunocytofluorescence. This suggests that the perinuclear iPLA$_2\beta$-immunoreactive proteins lack the region of sequence near the full-length iPLA$_2\beta$ N-terminus, and one such protein might be the 62 kDa caspase-3 cleavage product of iPLA$_2\beta$ (Figure 7A).

Cytofluorescence Studies of INS-1 Cells that Express iPLA$_2\beta$ as a Fusion Protein with EGFP. Immunocytofluorescence studies can be confounded by the cross reactivity of the antibody with proteins other than the intended target. Cytofluorescence studies (Figure 8) were therefore performed with INS-1 cells transfected with vectors (panel A) designed to produce EGFP alone (panels B and C), or iPLA$_2\beta$ as a fusion protein with the fluorescent EGFP tag at the N-terminus (EGFP-iPLA$_2\beta$, panels D and E) or at the C-terminus (iPLA$_2\beta$-EGFP, panels F and G). INS-1 cells that produced either iPLA$_2\beta$-EGFP or EGFP-iPLA$_2\beta$ develop apoptosis after induction of ER stress with thapsigargin (not shown).

Upon treatment with the vehicle (DMSO) for 6 h, INS-1 cells that produce EGFP alone (Figure 8, panel B), iPLA$_2\beta$-EGFP (panel D), or EGFP-iPLA$_2\beta$ (panel F) exhibit diffuse fluorescence with little evidence of compartmentalization. After induction of ER stress for 6 h with thapsigargin, INS-1 cells producing EGFP alone continue to exhibit diffuse fluorescence (panel C). The iPLA$_2\beta$-EGFP-producing cells, however, exhibit punctuate perinuclear fluorescence (panel E). In contrast, EGFP-iPLA$_2\beta$-producing cells exhibited diffuse cytoplasmic fluorescence after induction of ER stress,

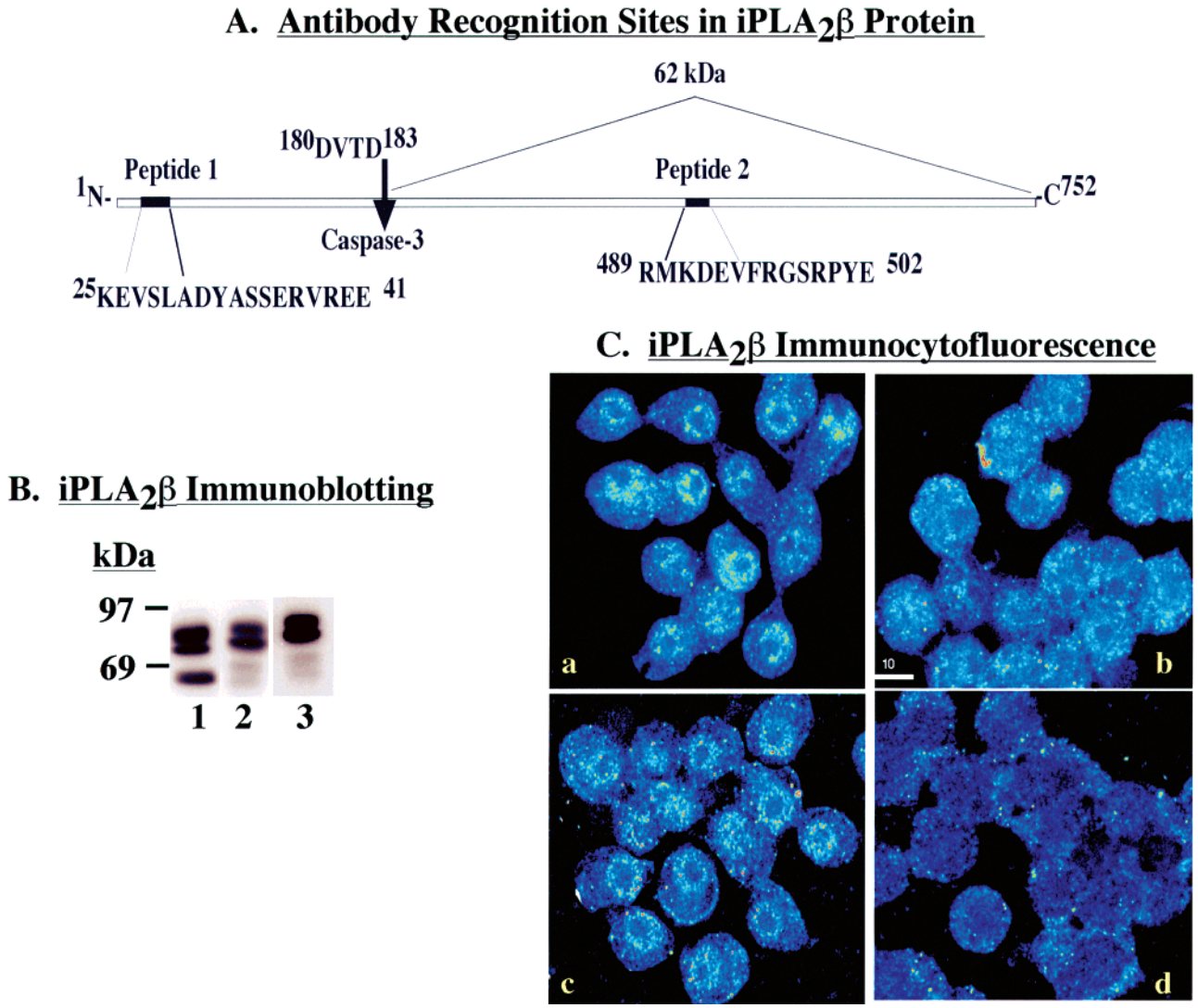

FIGURE 7: Characterization of the interaction of iPLA$_2\beta$-immunoreactive proteins with the iPLA$_2\beta$ antibody preparation. (A) iPLA$_2\beta$ protein schema. Illustration of peptide antigen sequences in iPLA$_2\beta$ against which antibodies were generated and location of the consensus sequence for caspase-3 cleavage. (B) Effects of caspase-3 inhibition on the generation of the 62 kDa iPLA$_2\beta$-immunoreactive protein postulated to arise from caspase-3 cleavage. The presence of the iPLA$_2\beta$-immunoreactive protein was examined in cytosol prepared from cells in the absence (lanes 1 and 3) or presence (lane 2) of a caspase-3 inhibitor (C3-I). Following SDS−PAGE analyses, the proteins were transferred to membranes for immunoblotting studies with the polyclonal iPLA$_2\beta$ antibody preparation in the absence (lanes 1 and 2) or presence of antigen peptide 2. (C) Fluorescence microscopy was used to visualize iPLA$_2\beta$ immunocytofluorescence in INS-1 cells probed with iPLA$_2\beta$ antibodies in the absence and presence of neutralizing peptide antigens: (a) iPLA$_2\beta$ antibodies alone, (b) iPLA$_2\beta$ antibodies with peptide 2, (c) iPLA$_2\beta$ antibodies with peptide 1, and (d) iPLA$_2\beta$ antibodies with peptides 1 and 2.

and there is no evidence of perinuclear localization (panel G). In fact, fluorescence was excluded from the nuclear region.

An interpretation of the findings illustrated in Figure 8 that is consistent with the scheme proposed in Figure 7A and with the discussion of findings in panels B and C of Figure 7 is that it is the C-terminal product of caspase-3 cleavage of iPLA$_2\beta$ that accumulates in the perinuclear region of INS-1 cells subjected to ER stress. This C-terminal product bears a fluorescent label when the substrate is iPLA$_2\beta$-EGFP but not when it is EGFP-iPLA$_2\beta$.

To determine whether inhibition of caspase-3 affects the subcellular redistribution of iPLA$_2\beta$-immunoreactive proteins induced by ER stress in INS-1 cells, the caspase-3 inhibitor C3-I was used in iPLA$_2\beta$ immunocytofluorescence studies of thapsigargin-treated cells (Figure 9). Compared to vehicle-treated control cells (Control panel) or to cells treated with C3-I alone (C3-I panel), INS-1 cells subjected to ER stress with thapsigargin in the absence of C3-I (T panel) exhibit intense perinuclear iPLA$_2\beta$ immunocytofluorescence, and this response is greatly attenuated by C3-I (T + C3-I panel). BEL does not affect the ER stress-induced perinuclear accumulation of iPLA$_2\beta$ immunoreactivity (not shown) under conditions where C3-I does so.

Inhibition of caspase-3 also greatly reduces the fraction of the INS-1 cell population that develops apoptosis after induction of ER stress (Figure 10), and the magnitude of this effect is similar to that observed with BEL (Figure 3B). The incidence of apoptosis in INS-1 cells treated with C3-I alone is similar to that exhibited by vehicle-treated cells (Figure 10). Taken together, the findings illustrated in Figures 5−10 suggest that ER stress in INS-1 cells induces the caspase-3-catalyzed cleavage of iPLA$_2\beta$ to yield a product that retains the native C-terminus, lacks a portion of the

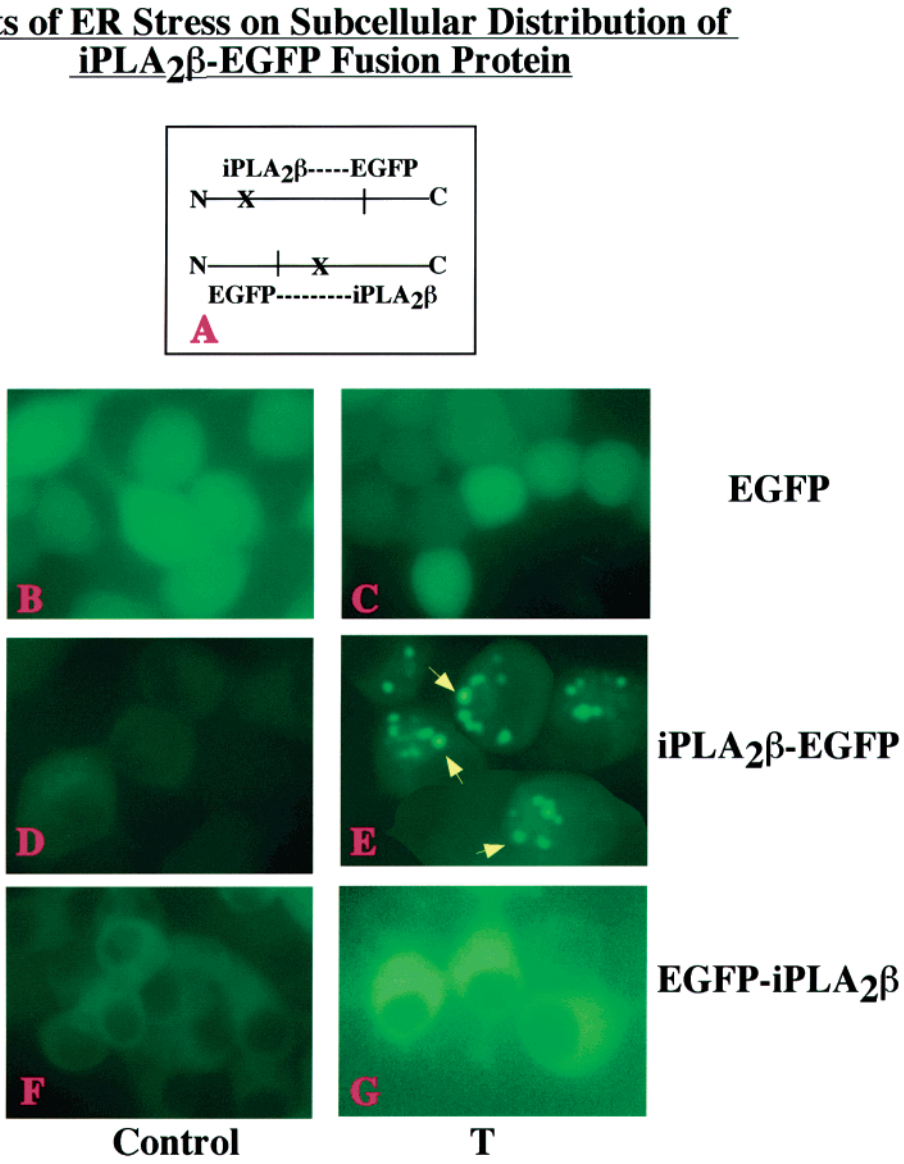

FIGURE 8: Effects of ER stress on the subcellular distribution of an iPLA$_2\beta$-EGFP fusion protein in INS-1 cells. (A) Schematic of two fusion protein constructs where X indicates the potential caspase-3 cleavage site in the iPLA$_2\beta$ protein. INS-1 cells were transfected with either EGFP vector alone (panels B and C) or constructs designed to attach the EGFP tag to the N-terminus (EGFP-iPLA$_2\beta$, panels D and E) or the C-terminus (iPLA$_2\beta$-EGFP, panels F and G) of iPLA$_2\beta$. Cells were treated with vehicle only (Control, panels B, D, and F) or with 1 μM thapsigargin (T, panels C, E, and G) and examined by fluorescence microscopy 6 h later. The iPLA$_2\beta$-EGFP-producing INS-1 cells treated with thapsigargin exhibit punctate perinuclear iPLA$_2\beta$ fluorescence, as indicated with yellow arrows (panel E).

native N-terminus, accumulates in the perinuclear region, retains catalytic activity, and plays a functional role in the development of apoptosis.

ER Stress-Induced Ceramide Accumulation in INS-1 Cells. Ceramide is an important lipid mediator of apoptosis (*49*−*51*), and recent reports suggest that iPLA$_2\beta$ activation promotes ceramide accumulation (*52*, *53*). We therefore examined whether ER stress-induced apoptosis is associated with ceramide accumulation in INS-1 cells and whether iPLA$_2\beta$ overexpression amplifies this response.

Ceramide (CM) species were measured as their Li^+ adducts (*42*) relative to the internal standard C8-CM, which contains an octanoic acid residue as the fatty amide substituent and is not an endogenous component of INS-1 cell lipids. Figure 11A is the positive ion ESI-MS total ion current (TIC) tracing of Li^+ adducts of the CM species in INS-1 cell lipids after addition of the C8-CM internal standard (IS), which is represented in the spectrum by its $[M + Li^+]^+$ ion (*m*/*z* 432). The fatty amide substituents of the major CM species endogenous to INS-1 cells are 24:0 (*m*/*z* 656), 24:1 (*m*/*z* 654), 22:0 (*m*/*z* 628), 18:0 (*m*/*z* 572), and 16:0 (*m*/*z* 544).

Panels B and C of Figure 11 are the tandem mass spectra produced by collisionally activated dissociation (CAD) of the $[M + Li^+]^+$ ions of C24:1-CM (*m*/*z* 654) and C16:0-CM (*m*/*z* 544), respectively. Both spectra contain prominent ($[M + Li^+]^+ - 48$) ions at *m*/*z* 606 (Figure 11B) and *m*/*z* 496 (Figure 11C), respectively, that reflect sequential neutral losses of water and form aldehyde (*42*). The two spectra contain the common ion at *m*/*z* 264 that arises from and identifies the long chain base (*42*). Ions that arise from and identify the fatty amide substituent (*42*) in Figure 11B include those at *m*/*z* 372 and 398, and analogous ions in Figure 11C occur at *m*/*z* 262 and 288. Formation of these ions is rationalized in Figure 11D.

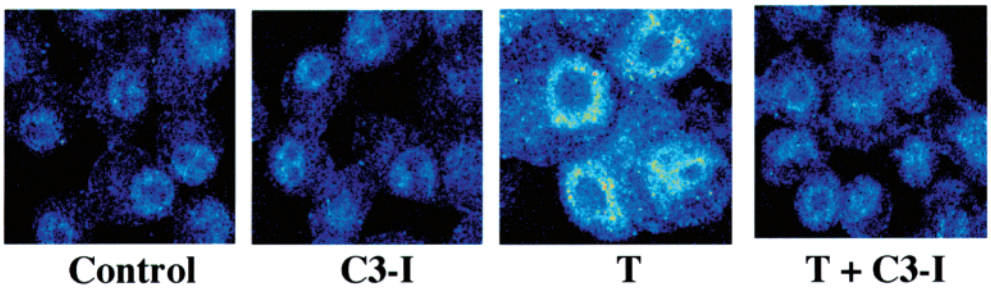

FIGURE 9: Effects of caspase-3 inhibition on the subcellular redistribution of iPLA$_2\beta$ immunocytofluorescence in INS-1 cells subjected to ER stress. OE cells were pretreated with vehicle alone or with caspase-3 inhibitor (C3-I, 500 nM) for 24 h. The vehicle-pretreated cells were then treated with vehicle alone (Control) or with 1 μM thapsigargin (T) alone, and the C3-I-pretreated cells were treated with C3-I alone (C3-I) or with T (T + C3-I). After an additional 24 h, the cells were processed for iPLA$_2\beta$ immunocytofluorescence analyses by fluorescence microscopy. The data are representative of findings obtained from three separate experiments.

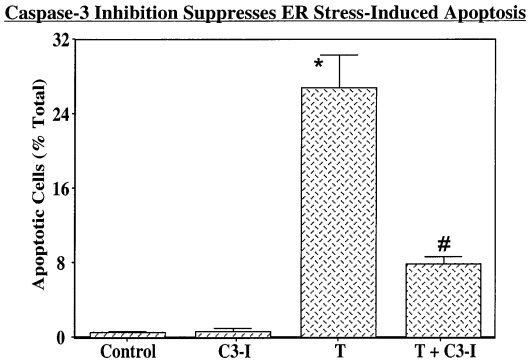

FIGURE 10: Effects of inhibition of caspase-3 on inhibition of ER stress-induced apoptosis of INS-1 cells. OE cells were pretreated with vehicle alone or with 500 nM C3-I for 24 h. The vehicle-pretreated cells were then treated with vehicle alone (Control) or with 1 μM thapsigargin (T) alone, and the C3-I-pretreated cells were treated with either C3-I alone (C3−I) or T (T + C3-I). After 24 h, cells were harvested and TUNEL analyses performed. The data representing the percentage of apoptotic cells, relative to the total number of cells, are illustrated as the mean ± SEM ($n = 10$). The asterisk denotes that the T group is significantly different from Control and C3-I groups and the pound sign that the T + C3-I group is significantly different from other groups ($p < 0.05$).

Figure 12 illustrates the application of monitoring a constant neutral loss (CNL) of 48 (*42*, *45*) to the measurement of CM species in INS-1 cells that overexpress iPLA$_2\beta$ after incubation for 24 h under control conditions (Figure 12A) or after induction of ER stress with thapsigargin (Figure 12B). In comparison to the abundances of CM species in control cells (Figure 12A), an increase in the abundance of all of the major endogenous CM species in the INS-1 cells subjected to ER stress (Figure 12B) is reflected by the increased intensity of ions that represent them (e.g., *m*/*z* 544, 572, 628, 654, and 656), relative to that for the C8-CM IS (*m*/*z* 432).

Figure 13 illustrates that ER stress-induced ceramide accumulation is time-dependent over 24 h and that this effect is much larger in stably transfected cells that overexpress iPLA$_2\beta$ (OE cells) than in INS-1 cells transfected with the empty retroviral vector (V cells). These findings suggest that enhanced ceramide accumulation might contribute to the stronger tendency of OE cells to undergo apoptosis in response to ER stress than V cells (Figure 3).

DISCUSSION

Apoptosis plays a prominent role in the loss of β-cells during development of type I diabetes (*6*), and type II diabetes is characterized by an initial peripheral insulin resistance and accompanying compensatory hyperinsulinemia that is followed by a loss in β-cell function and frank hyperglycemia (*4*, *5*). The progressive decrease in β-cell function in type II diabetes reflects, in part, β-cell death by apoptosis (*7*−*12*).

Three distinct recognized pathways for apoptosis include the (extrinsic) death receptor, the (intrinsic) mitochondrial, and the ER stress pathways (*23*, *24*, *43*, *54*, *55*). All three pathways result in activation of caspase-3 which is an executioner of apoptosis (*24*, *44*). ER stress-induced apoptosis has been reported to contribute to progressive β-cell death in the Akita diabetic mouse model (*56*) and to β-cell death induced by nitric oxide and the SERCA inhibitor thapsigargin (*57*, *58*), a known inducer of ER stress (*23*, *54*).

The potential deleterious effects of intracellular calcium store depletion on β-cell survival were previously also examined in MIN-6 insulinoma cells (*26*). In that study, depletion of ER calcium stores in MIN-6 insulinoma cells by thapsigargin was found to induce apoptosis by a mechanism that does not require an increase in the intracellular calcium concentration, but that does require generation of the arachidonic acid 12-lipoxygenase product 12-HETE (*26*). This implies that thapsigargin induces β-cell hydrolysis of arachidonic acid from membrane phospholipids by a mechanism that does not require a rise in the cytosolic Ca^{2+} concentration, and this has been demonstrated to occur in pancreatic islets (*27*) by a pathway that is suppressed by BEL, a suicide substrate inhibitor of the group VIA phospholipase A_2 (iPLA$_2\beta$). Similarly, the cytokine IL-1 induces β-cell NO production and apoptosis and hydrolysis of arachidonic acid from membrane phospholipids by a mechanism that is also sensitive to inhibition by BEL (*59*). These observations suggest that iPLA$_2\beta$ might participate in membrane phospholipid hydrolysis in β-cells in which apoptosis is induced by exposure to IL-1 or induction of ER stress.

The possibility that iPLA$_2\beta$ participates in ER stress-induced apoptosis was examined here in iPLA$_2\beta$-expressing (*32*, *33*, *45*, *46*) INS-1 insulinoma cells, and the findings

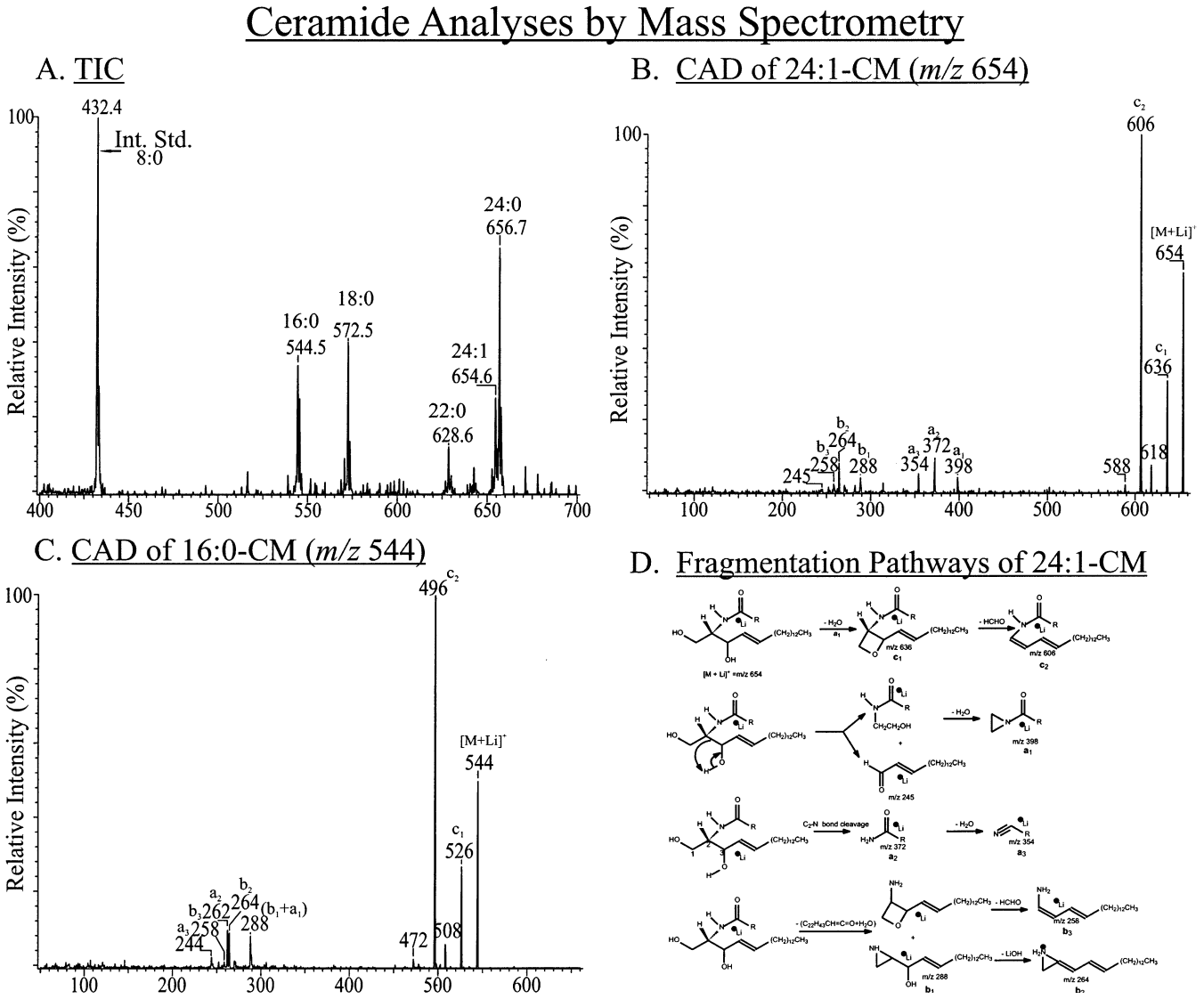

FIGURE 11: Electrospray ionization (ESI) mass spectrometric analyses of ceramide species from INS-1 cells as Li^+ adducts. Ceramides were extracted from INS-1 cells and analyzed by ESI/MS as Li^+ adducts. (A) Positive ion ESI/MS total ion current (TIC). (B) ESI/MS tandem spectrum obtained from collisionally activated dissociation (CAD) of *m*/*z* 654 (C24:1−CM−Li^+). (C) ESI/MS tandem spectrum obtained from CAD of *m*/*z* 544 (C16:0−CM−Li^+). (D) Rationalization of the ceramide (24:1-CM) fragmentation pattern. R is the fatty acid substituent side chain.

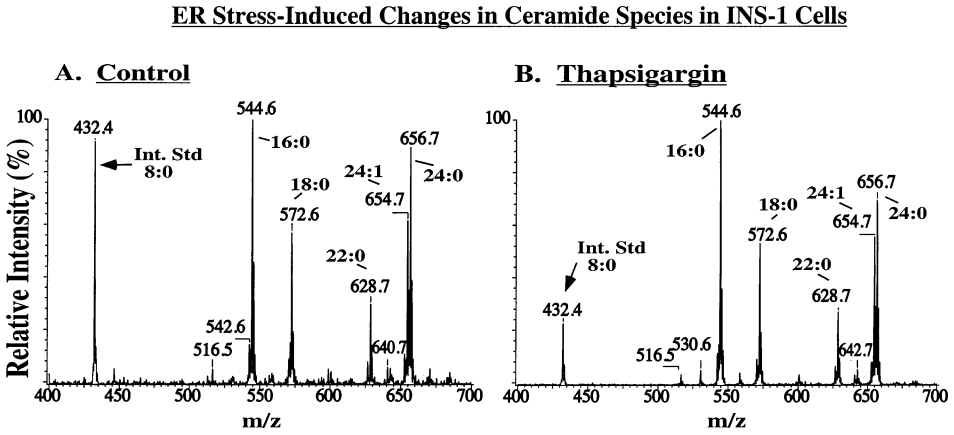

FIGURE 12: ER stress-induced ceramide accumulation in INS-1 cells. Ceramides extracted from OE cells incubated for 24 h with vehicle alone (A) or with thapsigargin (B) were analyzed as Li^+ adducts by ESI/MS/MS scanning for a constant neutral loss of 48.

reveal that induction of ER stress in parental INS-1 cells with thapsigargin induces apoptosis, and that BEL suppresses this response in a concentration-dependent manner. This is consistent with a role for iPLA$_2\beta$ in ER stress-induced β-cell apoptosis. Supporting this role for iPLA$_2\beta$ is the finding that anti-Fas antibody-induced apoptosis of human promonocytic

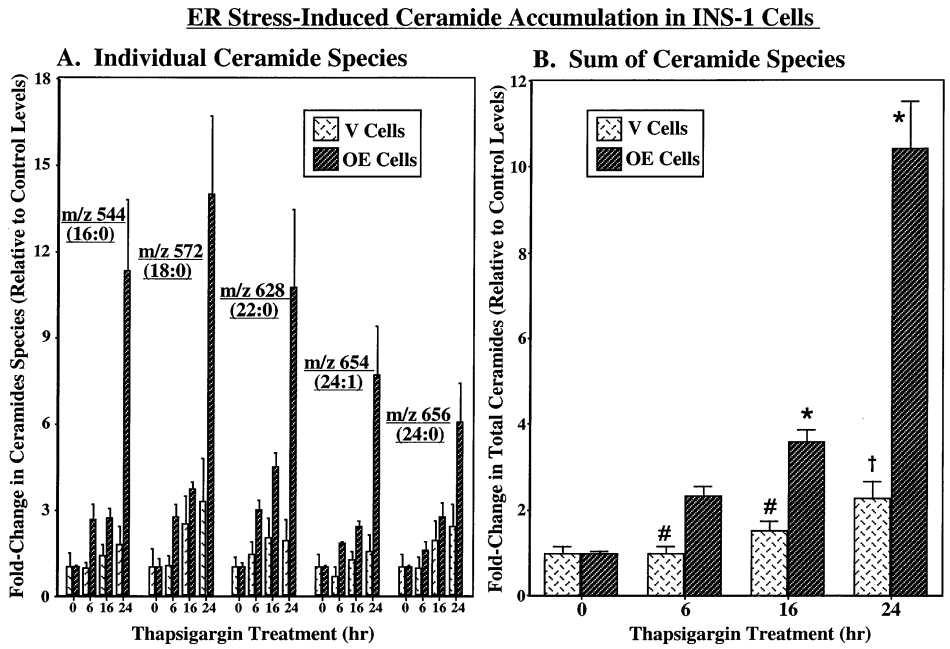

FIGURE 13: Time-course of ER stress-induced ceramide accumulation in INS-1 cells and effects of iPLA$_2\beta$ overexpression. The ceramide (CM) content was measured by ESI/MS/MS in lipids extracted from INS-1 cells transfected with the empty vector (V cells) or stably transfected INS-1 cells that overexpress iPLA$_2\beta$ (OE cells) treated for various periods with thapsigargin (1 μM). The CM content was normalized to the total lipid phosphorus content and expressed as the ratio to the normalized CM content of the time zero value. (A) Change in content with time after exposure to thapsigargin for individual CM molecular species. (B) Time course of accumulation of the sum of all CM species. The asterisks denote that thapsigargin-treated OE-cell groups are significantly different from the corresponding 0 h OE group ($p < 0.01$). The dagger denotes that the V cell group at 24 h is significantly different from the corresponding 0 h V cell group and OE group at 24 h ($p < 0.05$). The pound signs denote that the V cell groups at 6 and 16 h are significantly different from the corresponding OE groups ($p < 0.05$).

U937 cells is associated with release of arachidonic acid that is not mediated by cPLA$_2$ or sPLA$_2$ but is inhibited by BEL (*28*).

Our finding that ER stress-induced apoptosis of INS-1 cells is suppressed by BEL caused us to determine whether overexpression of iPLA$_2\beta$ in INS-1 cells would affect their sensitivity to ER stress. Overexpression of iPLA$_2\beta$ did amplify the INS-1 cell apoptotic response to thapsigargin, and this response is also suppressed by BEL. In addition, thapsigargin-induced apoptosis of INS-1 cells is associated with stimulation of iPLA$_2\beta$ activity within 1 h of exposure, and the enzymatic activity continues to increase for 12 h. Moreover, enzymatic, immunoblotting, and immunocytofluorescence analyses all demonstrate a thapsigargin-induced perinuclear accumulation of iPLA$_2\beta$ protein and enzymatic activity and the accumulation of a 62 kDa iPLA$_2\beta$-immunoreactive protein in the nuclear fraction.

Caspase-3-catalyzed cleavage of iPLA$_2\beta$ at its ^{180}DVTD^{183} consensus site (*29*, *44*) would yield a 62 kDa product that retains the ^{462}GTSTG^{466} lipase catalytic center and lacks a region of N-terminal sequence that includes one of the two antigenic peptide sites (peptide 1) recognized by our iPLA$_2\beta$ antibody preparation. Such a 62 kDa product would retain the other antigenic peptide site (peptide 2). Consistent with an origin of the INS-1 cell 62 kDa iPLA$_2\beta$-immunoreactive protein from caspase-3 action, peptide 2, but not peptide 1, blocks recognition of this immunoreactive protein by the iPLA$_2\beta$ antibody. In addition, inhibition of caspase-3 activity reduces the level of perinuclear accumulation of iPLA$_2\beta$ immunocytofluorescence, generation of 62 kDa iPLA$_2\beta$-immunoreactive band, and nuclear accumulation of iPLA$_2\beta$ enzymatic activity. These findings suggest induction of ER stress with thapsigargin promotes caspase-3-catalyzed cleavage of INS-1 cell iPLA$_2\beta$.

The caspase-3 inhibitor also reduces INS-1 cell apoptosis following thapsigargin treatment, consistent with the recognized role of caspase-3 as an executioner of apoptosis (*24*, *44*). Induction of apoptosis in human promonocytic U937 cells is also associated with caspase-3-catalyzed cleavage of iPLA$_2\beta$ (*29*), and overexpression of this truncated form (amino acid 184 $\rightarrow$ C-terminus) of iPLA$_2\beta$ in human embryonic kidney cells enhances both apoptosis and AA release (*29*). These findings suggest that the product of caspase-3-catalyzed iPLA$_2\beta$ is more active than the full-length iPLA$_2\beta$, and it has been suggested that the more active shorter iPLA$_2\beta$ isoform hydrolyzes nuclear membrane phospholipids, which disrupts membrane fluidity and results in apoptosis. Though BEL was effective in suppressing iPLA$_2\beta$ activity over the study period following thapsigargin treatment, it did not appear to attenuate perinuclear accumulation of the iPLA$_2\beta$ protein or significantly inhibit generation of a 62 kDa iPLA$_2\beta$-immunoreactive product. These observations suggest that BEL is affecting iPLA$_2\beta$ downstream of caspase-3. Our findings that thapsigargin stimulates iPLA$_2\beta$ activity and promotes caspase-3-catalyzed cleavage of INS-1 cell iPLA$_2\beta$ and accumulation of the resultant 62 kDa iPLA$_2\beta$-immunoreactive product in the perinuclear region suggest that these events may be involved in the mechanism by which iPLA$_2\beta$ participates in ER stress-induced β-cell apoptosis.

INS-1 cells that overexpress iPLA$_2\beta$ also accumulate larger amounts of ceramide when treated with thapsigargin than do control INS-1 cells. Ceramides are lipid messengers that suppress cell growth and induce apoptosis (*49*−*51*). They

can be generated via sphingomyelin hydrolysis by sphingomyelinase, resulting in the generation of ceramide and phosphocholine (*60*) or by *de novo* synthesis from palmitate (16:0) and other precursors. This latter mechanism is thought to be involved in lipoapoptosis of β-cells (*61*). Ceramide accumulation can also result from degradation of ceramidase, a pathway that is promoted by nitric oxide (*52*). Increases in the level of ceramide generation have been linked to arachidonic acid levels in colorectal cancer cells and HL-60 cells (*62*, *63*), and IL-1β-induced arachidonic acid generation from pancreatic islets has been shown to be sensitive to inhibition by BEL (*59*). Taken together with the recent demonstration that LPS-induced generation of nitric oxide is inhibited by BEL (*53*), these findings raise the possibility that iPLA$_2\beta$ activation could enhance NO production and cause degradation of ceramidase, accumulation of ceramide, and amplification of apoptosis.

ER stress-induced β-cell apoptosis is now thought to be a potentially important factor in the development of diabetes (*58*). As membranes of the nucleus and ER are contiguous (*64*, *65*), perinuclear accumulation of iPLA$_2\beta$ is consistent with association of the iPLA$_2\beta$ protein with a subcellular compartment that is likely to include ER (*64*). The β-cell ER is enriched in arachidonate-containing plasmenylethanolamine species (*40*), and products of PLA$_2$ action might participate in apoptosis, as has been previously suggested (*26*, *59*, *66*−*68*). Our findings support the possibility that iPLA$_2\beta$ and the products of its action participate in β-cell apoptosis.

ACKNOWLEDGMENT

We thank Ms. Karen Greene and Dr. Mary Wohltmann for their expert technical assistance.

REFERENCES

1. Didac, M., and Mandrup-Poulsen, T. (1998) *Diabetes 47*, 1537−1543.
2. Eizirik, D. L., and Mandrup-Poulsen, T. (2001) *Diabetologia 44*, 2115−2133.
3. Tisch, R., and McDevitt, H. (1996) *Cell 85*, 291−297.
4. Kahn, C. R. (1995) *Nature 373*, 384−385.
5. De Fronzo, R. A. (1997) *J. Clin. Invest. 5*, 177−269.
6. Mathis, D., Vence, L., and Benoist, C. (2001) *Nature 414*, 792−798.
7. Cerasi, E., Kaiser, N., and Leibowitz, G. (2000) *Diabetes Metab. 26*, 13−16.
8. Chandra, J., Zhivotovsky, B., Zaitsev, S., Juntti-Berggrren, L., Berggren, P. O., and Orrenius, S. (2001) *Diabetes 50*, S44−S47.
9. Donath, M. Y., Gross, D. J., Cerasi, E., and Kaiser, N. (1999) *Diabetes 48*, 738−744.
10. Koyama, M., Wads, R., Sakurba, H., Mizukami, H., and Yagihashi, S. (1998) *Am. J. Pathol. 153*, 537−545.
11. Mandrup-Poulsen, T. (2001) *Diabetes 50*, S58−S63.
12. Sesti, G. (2002) *Ann. Med. 34*, 444−450.
13. Ludvik, B., Nolan, J. J., Baloga, J., Sacks, D., and Olefsky, J. (1995) *Diabetes 44*, 1121−1125.
14. Polonsky, K. S. (2000) *Int. J. Obes. Relat. Metab. Disord. 24*, S29−S31.
15. Flier, S. N., Kulkarami, R. N., and Kahn, C. R. (2001) *Proc. Natl. Acad. Sci. U.S.A. 98*, 7475−7480.
16. Ogilvie, R. F. (1993) *J. Pathol. 37*, 473−481.
17. Kloppel, G., Mattias, L., Habich, K., Oberholzer, M., and Heitz, P. U. (1985) *Surv. Synth. Pathol. Res. 4*, 110−125.
18. Clark, A., Wells, C. A., Buley, I. D., Cruickshank, J. K., Vanhegan, R. I., Mathews, D. R., Copper, G. J. S., Holman, R. R., and Turner, R. C. (1988) *Diabetes Res. 9*, 151−159.
19. Stefan, Y., Orci, L., Malaisse-Lagae, F., Perrelet, A., Patel, Y., and Unger, R. H. (1982) *Diabetes 3*, 694−700.
20. Pick, A., Clark, J., Kubstrup, C., Levisetti, M., Pugh, W., Bonner-Weir, S., and Polonsky, K. (1998) *Diabetes 47*, 358−364.
21. Butler, A. E., Janson, J., Bonner-Weir, S., Ritzel, R., Rizza, R. A., and Butler, P. C. (2003) *Diabetes 52*, 102−110.
22. Oyadomari, S., Araki, E., and Mori, M. (2002) *Apoptosis 7*, 335−345.
23. Diaz-Horta, O., Kamagate, A., Herchuelz, A., and Van Eylen, F. (2002) *Diabetes 51*, 1815−1824.
24. Mehmet, H. (2000) *Nature 403*, 29−30.
25. Thastrup, O., Cullen, P. J., Drobak, B. K., Hanley, M. R., and Dawson, A. P. (1990) *Proc. Natl. Acad. Sci. U.S.A. 87*, 2466−2470.
26. Zhou, Y.-P., Teng, D., Dralyuk, F., Ostrega, D., Roe, M. W., Phillipson, L., and Polonsky, K. (1998) *J. Clin. Invest. 101*, 1623−1632.
27. Nowatzke, W., Ramanadham, S., Ma, Z., Hsu, F.-F., Bohrer, A., and Turk, J. (1998) *Endocrinology 139*, 4073−4085.
28. Atsumi, G., Tajima, M., Hadano, A., Nakatani, Y., Murakami, M., and Kudo, I. (1998) *J. Biol. Chem. 273*, 13870−13877.
29. Atsumi, G., Murakami, M., Kojima, K., Hadano, A., Tajima, M., and Kudo, I. (2000) *J. Biol. Chem. 275*, 18248−18258.
30. Coffin, J. M., and Hart, G. W. (1996) in *Retrovirus*, Cold Spring Harbor Laboratory Press, Plainview, NY.
31. Ma, Z., Ramanadham, S., Kempe, K., Chi, X. S., Ladenson, J. L., and Turk, J. (1997) *J. Biol. Chem. 272*, 11118−11127.
32. Ma, Z., Ramanadham, S., Bohrer, A., Wohltmann, M., Zhang, S., and Turk, J. (2001) *J. Biol. Chem. 276*, 13198−13208.
33. Ma, Z., Zhang, S., Turk, J., and Ramanadham, S. (2002) *Am. J. Physiol. 282*, E820−E833.
34. Cormack, B. P., Valdivia, R., and Falkow, S. (1996) *Gene 173*, 33−38.
35. Gross, R. W., Ramanadham, S., Kruszka, K., Han, X., and Turk, J. (1993) *Biochemistry 32*, 327−336.
36. Ramanadham, S., Bohrer, A., Gross, R. W., and Turk, J. (1993) *Biochemistry 32*, 13499−13509.
37. Smith, L. (1955) Spectrophotometric assay of cytochrome C oxidase, in *Methods of Biochemical Analysis* (Glick, D., Ed.) Vol. II, pp 427, Wiley-Interscience, New York.
38. Ramanadham, S., Gross, R. W., Han, X., and Turk, J. (1993) *Biochemistry 32*, 337−346.
39. Ramanadham, S., Wolf, M. J., Li, B., Bohrer, A., and Turk, J. (1997) *Biochim. Biophys. Acta 1344*, 153−164.
40. Ramanadham, S., Wolf, M. J., Jett, P. A., Gross, R. W., and Turk, J. (1994) *Biochemistry 33*, 7442−7452.
41. Hsu, F.-F., and Turk, J. (2002) *J. Am. Soc. Mass Spectrom. 13*, 558−570.
42. Hsu, F.-F., Turk, J., Stewart, M. E., and Downing, D. T. (2002) *J. Am. Soc. Mass Spectrom. 13*, 680−695.
43. Bitko, V., and Barik, S. (2001) *J. Cell. Biochem. 80*, 441−454.
44. Cohen, G. M. (1997) *Biochem. J. 326*, 1−16.
45. Ramanadham, S., Hsu, F.-F., Bohrer, A., Ma, Z., and Turk, J. (1999) *J. Biol. Chem. 274*, 13915−13927.
46. Ma, Z., Bohrer, A., Wohltmann, M., Ramanadham, S., Hsu, F.-F., and Turk, J. (2001) *Lipids 36*, 689−700.
47. Balsinde, J., and Dennis, E. A. (1996) *J. Biol. Chem. 271*, 31937−31941.
48. Balboa, M. A., Balsinde, J., and Dennis, E. A. (1998) *J. Biol. Chem. 273*, 7684−7690.
49. Jayadev, S., Liu, B., Bielawska, A. E., Lee, J. Y., Nazaire, F., Pushkareva, M. Yu., Obeid, L. M., and Hannun, Y. A. (1995) *J. Biol. Chem. 270*, 2047−2052.
50. Obeid, L. M., and Hannun, Y. A. (1995) *J. Cell. Biochem. 58*, 191−198.
51. Venable, M. E., Lee, J. Y., Smyth, M. J., Bielawska, A., and Obeid, L. M. (1995) *J. Biol. Chem. 270*, 30701−30708.
52. Franzen, R., Fabbro, D., Aschrafi, A., Pfeilschifter, J., and Huwiler, A. (2002) *J. Biol. Chem. 277*, 46184−46190.
53. Vivancos, M., and Moreno, J. J. (2002) *Nitric Oxide 6*, 255−262.
54. Nakagawa, T., Zhu, H., Morishima, N., Li, E., Xu, J., Yankner, B. A., and Yuan, J. (2000) *Nature 403*, 98−103.
55. Rao, R. V., Castro-Obregon, S., Frankowski, H., Schuler, M., Stoka, V., del Rio, G., Bredesen, D. E., and Ellerby, H. M. (2002) *J. Biol. Chem. 277*, 21836−21842.
56. Oyadomari, S., Koizumi, A., Takeda, K., Gotoh, T., Akira, S., Araki, E., and Mori, M. (2002) *J. Clin. Invest. 109*, 525−532.
57. Oyadomari, S., Takeda, K., Takiguchi, M., Gotoh, T., Matsumoto, M., Wada, I., Akira, S., Akira, S., Araki, E., and Mori, M. (2001) *Proc. Natl. Acad. Sci. U.S.A. 98*, 10845−10850.

58. Oyadomari, S., Araki, E., and Mori, M. (2002) *Apoptosis 7*, 335−345.
59. Ma, Z., Ramanadham, S., Corbett, J. A., Bohrer, A., Gross, R. W., McDaniel, M. L., and Turk, J. (1996) *J. Biol. Chem. 271*, 1029−1042.
60. Hannun, Y. A. (1994) *J. Biol. Chem. 269*, 3125−3128.
61. Shimabukuro, M., Higa, M., Zhou, Y.-T., Wang, M.-Y., Newgard, C. B., and Unger, R. H. (1998) *J. Biol. Chem. 273*, 32487−32490.
62. Chan, T. A., Morin, P. J., Vogelstein, B., and Kinzler, K. W. (1998) *Proc. Natl. Acad. Sci. U.S.A. 95*, 681−686.
63. Surette, M. E., Fonteh, A. N., Bernatchez, C., and Chilton, F. H. (1999) *Carcinogen 20*, 757−763.
64. Holz, G. G., Leech, C. A., Heller, R. S., Castonguay, M., and Habener, J. F. (1999) *J. Biol. Chem. 274*, 14147−14156.
65. Schievella, A. R., Regiers, M. K., Smith, W. L., and Lin, L. L. (1995) *J. Biol. Chem. 270*, 30749−30754.
66. Bleich, D., Chen, S., Zipser, B., Sun, D., Funk, C., and Nadler, J. (1999) *J. Clin. Invest. 103*, 1431−1436.
67. Flodstrom, M., Tyrberg, B., Eizirik, D. L., and Sandler, S. (1999) *Diabetes 48*, 706−713.
68. Mirzoeva, O. K., Yaqoob, P., Knox, K. A., and Calder, P. C. (1996) *FEBS Lett. 396*, 266−270.

BI035536M